Non-linear high Tg polyimide-based membranes for separating CO_2/CH_4 gas mixtures

Madzarevic, Zeljka P.; Seoane, Beatriz; Gascon, Jorge; Hegde, Maruti; Dingemans, Theo J.

DOI
10.1016/j.polymer.2022.125520

Publication date
2022

Document Version
Final published version

Published in
Polymer

Polymer 263 (2022) 125520

Contents lists available at ScienceDirect

Polymer

journal homepage: www.elsevier.com/locate/polymer

Non-linear high Tg polyimide-based membranes for separating CO_2/CH_4 gas mixtures

Zeljka P. Madzarevic [a,b], Beatriz Seoane [c], Jorge Gascon [d], Maruti Hegde [e], Theo J. Dingemans [e,*]

[a] Faculty of Aerospace Engineering, Novel Aerospace Materials, Delft University of Technology, Kluyverweg 1, 2629HS, Delft, the Netherlands
[b] Dutch Polymer Institute (DPI), P.O. Box 902, 5600AX, Eindhoven, the Netherlands
[c] Faculty of Applied Sciences, Catalysis Engineering-Chemical Engineering Department, Delft University of Technology, Julianalaan 136, 2628BL, Delft, the Netherlands
[d] King Abdullah University of Science and Technology, KAUST Catalysis Center, Advanced Catalytic Materials, Thuwal, 23955, Saudi Arabia
[e] University of North Carolina at Chapel Hill, Department of Applied Physical Sciences, Murray Hall 1113, 121 South Road, NC, 27599-3050, USA

ARTICLE INFO

Keywords:
Polyimide
Membrane
Gas separation
Mixed gases

ABSTRACT

A novel series membranes based on non-linear all-aromatic polyimides (PIs) was investigated with the aim to understand how the PI backbone geometry and local electrostatics govern gas transport and the ability to separate CO_2/CH_4 mixtures. Non-linear 3-ring aromatic diamines, with exocyclic bond angles varying between 120 and 134°, enable the design of high Tg (>276 °C) PIs. A polar 1,3,4-oxadiazole diamine (ODD) (μ = 3D) monomer and a non-polar *m*-terphenyl diamine (TPD) reference monomer were synthesized and coupled with 3 dianhydrides, *i.e.* ODPA, ODDA, and 6FDA. In 6FDA-based membranes CO_2 permeabilities (P_{CO2}) are the highest of the series. The 6FDA-ODD membrane shows excellent membrane performance with high P_{CO2} values at all feed pressures. Up to 12 bar (6 bar CO_2) none of the membranes reached their plasticization pressure. The non-linear backbone geometry promotes CO_2 permeability, whereas the presence of an electrostatic dipole moment associated with the 1,3,4-oxadiazole heterocycle governs CO_2/CH_4 separation selectivity.

1. Introduction

The development of polyimide (PI) gas separation membranes has been hindered by their inherent trade-off between the gas permeability and the separation selectivity [1,2]. The way to achieve high permeability as well as high selectivity, in all-aromatic polyimides as dense glassy membranes, is through a careful structure/property optimization process. The gas separating properties of dense glassy polymeric membranes are very sensitive to the chemical structure of the repeating units, with permeability coefficients for CO_2 in different polymer classes varying over 8 orders of magnitude from 3×10^{-4} Barrer [3] to 2.7×10^4 Barrer [4,5].

Theoretical and empirical studies have shown that by incorporating bulky pendant groups both permeability and selectivity can be controlled [6–8]. Bulky pendant groups such as trimethylsilyl, fluorenyl, phenyl or *t*-butyl groups inhibit chain packing efficiency consecutively increasing free volume and therefore enhancing permeability, while maintaining high selectivity [6,9]. The most permeable glassy polymers are those that possess the highest free volume due to the presence of intermolecular voids within a material [10,11]. Free volume can be trapped in the solid state during membrane preparation when the polymer backbone contains bulky pendant groups or groups that introduce steric hindrance and frustrate chain packing thereby increasing the average interchain spacing. One well-known modification is the hexafluoro propane linker –$C(CF_3)_2$-, present in 2,2′-bis(3,4-carboxylphenyl) hexafluoropropane dianhydride (6FDA). This dianhydride has been a popular monomer in many polyimide membrane studies [9,12–16]. Having this in mind, another aspect we set-off to investigate is the role of heterocyclic (heteroaromatic) moieties in the polyimide backbone. Even though a great deal of research has been published on the role of polyimide main-chain structure on gas separation performance, understanding the role of heterocyclic building blocks is still lacking. Heterocycles are inherent to the backbone of aromatic polyimides, but in order to further increase their content, Sen et al. [14] included pyridine and thiophene in the polyetherimide (PEI) backbone. Their results show that the enhanced polarity of heterocyclic groups (e.g. pyridine and thiophene) in the PEI backbone increases the permeability of CO_2 by 60% for the pyridine-containing PEI and by 36% for the thiophene-containing PEI, while maintaining a similar CO_2/CH_4 selectivity found in the linear PEI analogs.

* Corresponding author.
E-mail address: tjd@unc.edu (T.J. Dingemans).

https://doi.org/10.1016/j.polymer.2022.125520
Received 7 August 2022; Received in revised form 10 November 2022; Accepted 13 November 2022
Available online 16 November 2022

In this paper we present a new series of PIs, in which we have explored novel diamine monomers that introduce non-linearity (prevent crystallization) and at the same time increase the concentration of electrostatic dipole moments per polymer repeat unit. We synthesized 6 PIs, Fig. 1, that are based on a polar 2,5-bis(4-aminophenyl)-1,3,4-oxadiazole (ODD) monomer and its non-polar analog 4,4″-diamino-*m*-terphenyl (TPD).

Oxadiazole was chosen because of the favorable properties displayed by polyoxadiazoles and oxadiazole-based polymer membranes such as a high CO_2/CH_4 selectivity, a high T_g (low intersegmental mobility) and chemical stability to a broad range of fluids and gasses [8,14]. Both diamines are *para*-substituted with respect to the central ring, and ODD brings a strong lateral dipole moment of 3 Debye associated with its central oxadiazole ring while TPD has no dipole moment [17]. Changing the exocyclic bond angle in these 3-ring diamines, from 134° for ODD to 120° for TPD subtly modifies the (non-polar) geometry to a more bent or kinked conformation, which is likely to increase the free volume in the polymers. With respect to the dianhydrides, we have selected 2,2′-bis(3,4-carboxylphenyl)hexafluoropropane dianhydride (6FDA) as a well-known dianhydride with excellent gas separation performance. 6FDA is a rather stiff monomer, its $-CF_3$ groups inhibit rotations thereby increasing rigidity and free volume. Furthermore, we investigated 3,3′,4,4′-oxydiphthalic dianhydride (ODPA), which has shown promising membrane performance in our previous series [18]. We have synthesized 4,4'-(1,3,4-oxadiazole-2,5-diyl)diphthalic anhydride (ODDA), in order to learn more about non-linear PIs with two strong lateral dipole moments in the polymer backbone (ODDA-ODD). A Matrimid® membrane was used as a reference material.

2. Experimental

2.1. Materials

Monomer 2,5-bis(4-aminophenyl)-1,3,4-oxadiazole (ODD) was previously synthesized according to a procedure reported by Grucela-Zajac et al. [19] Monomers 4,4″-diamino-*m*-terphenyl (TPD) and 4,4'-(1,3,4-oxadiazole-2,5-diyl)diphthalic anhydride (ODDA) were synthesized according to literature procedures [20,21]. All start materials were purchased from commercial sources and used as received unless stated otherwise. Dianhydrides 6FDA and ODPA were purchased from TCI Co. Ltd. and were dried overnight prior to use in a vacuum oven at 60 °C. N-Methyl-2-pyrrolidinone (NMP) was obtained from Acros Organics. Matrimid® 5218 was supplied by Huntsman Advanced Materials in the form of a soluble fully imidized polyimide powder and was dried for 48 h under vacuum at 150 °C prior to use.

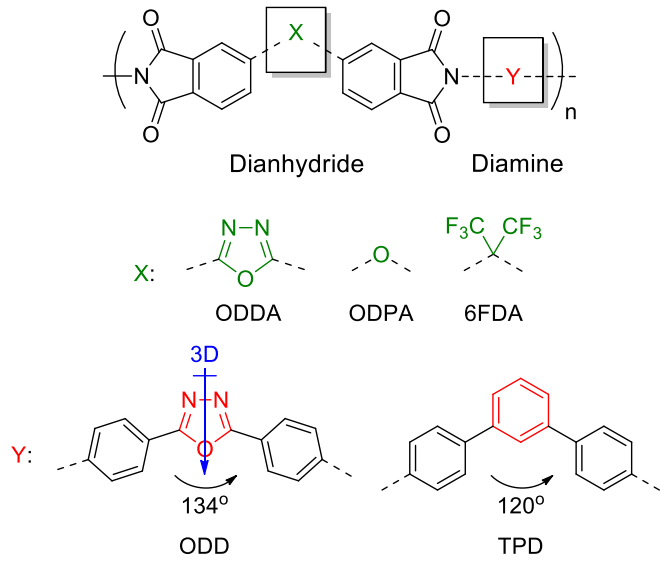

Fig. 1. Chemical structures of the non-linear polyimides. Structures of the dianhydrides are shown in green. The core structures of diamines are in red, with the oxadiazole core having an exocyclic bond angle of 134° whereas the *m*-terphenyl diamine has an exocyclic bond angle of 120°. The oxadiazole core in ODD has a transverse dipole moment of 3 Debye whereas TPD is non-polar. (For interpretation of the references to color in this figure legend, the reader is referred to the Web version of this article.)

2.2. Characterization

The structures of the TPD and ODDA monomers were confirmed by ^{1}H NMR (Agilent-400 MR DD2, 400 MHz) and ^{13}C NMR (Agilent-400 MR DD2, 100 MHz). All samples were dissolved in dimethyl sulfoxide-d6 and the recorded spectra were referenced to the solvent (DMSO-d_6: ^{1}H 2.50 and ^{13}C 39.5 ppm) relative to TMS.

For GC/MS analysis of TPD, a Shimadzu GCMS-QP2010S gas chromatograph mass spectrometer was used coupled with the GL Sciences Optic 3 high-performance injector. Separation of the evolved gases was achieved using a 30 m × 0.025 mm SGE forte BPX-5 capillary column operated at a He flow rate of about 1 mL/min. Software ATAS Evolution Workstation (ATAS GL International) controlled heating of the injection port of the GC from 50 °C to 300 °C in 5 min. The GC column oven was programmed from 50 °C, with a heating rate of 20 °C/min, to 300 °C (held for 30 min). LabSolutions data system, GCMSsolutions (Shimadzu) Postrun analysis software was used to integrate the peaks.

Gel permeation chromatography (GPC) measurements of the polyamic acids were performed on a Shimadzu Prominence GPC system equipped with two Shodex LF-804 columns. N-Methyl-2-pyrrolidone (NMP) with 5 mM of LiBr was used as eluent at a flow rate of 0.5 mL/min at 60 °C. Data analyses were performed with LabSolutions software using the refractive index detector data. Quantification was made based on polystyrene standard calibration. All polyamic solutions were filtered through a 0.45 μm PTFE filter prior to a GPC run.

Thermogravimetric analysis (TGA) was performed on a PerkinElmer Pyris diamond TG/DTA under a nitrogen atmosphere and a scan rate of 10 °C/min. Melting points of monomers and thermal properties of the PI films were determined by differential scanning calorimetry using a PerkinElmer Sapphire DSC. A heating rate 20 °C/min was used and all measurements were performed under a nitrogen atmosphere. Polymer thin films were investigated using a dynamic mechanical thermal analyzer (DMTA) in the temperature range 0 °C–400 °C, at a heating rate of 2.5 °C/min and at a frequency of 1 Hz, under a nitrogen atmosphere. Approximate dimensions of films were 20 × 4 × 0.03 mm. All samples were dried in a vacuum oven at 60 °C for 1 h prior to testing.

To investigate the morphology of the PI films (thickness of 19–38 μm), XRD experiments were conducted using a Bruker AXS D8 Advance X-ray diffractometer in reflection mode (Bragg Brentano geometry), with cobalt as the radiation source and a LynxEye detector. For every PI film, three layers were fixed onto a silicon wafer support with Scotch tape. All experiments were performed at room temperature in the 2θ range from 5° to 50°, with step size of 0.04° at 0.8 s per step.

2.3. Monomer synthesis

Terphenyl diamine (TPD) was synthesized using Suzuki-Miyara aryl–aryl coupling conditions, the synthesis is a modified procedure of what was reported by Sinclair and Sherburn [20]. Our two-step procedure is shown in Scheme 1 and the synthetic details are described in more detail bellow.

4,4″-Dinitro-m-terphenyl. A 1000 mL three-neck round-bottomed flask, equipped with an argon gas inlet tube, a reflux condenser, and a magnetic stirrer, was charged with 5 g (0.030 mol) of 1,3-benzenediboronic acid, 12.19 g (0.060 mol) of 1-bromo-4-nitrobenzene, 60 mL of 2 M K_2CO_3 solution and 300 ml of THF. This mixture was stirred under a slight argon over pressure. After 1 h, 0.349 g (1 mol%) of tetrakis

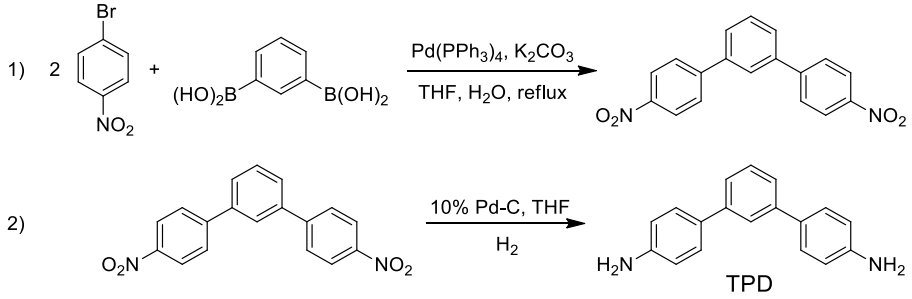

Scheme 1. Synthesis of 4,4″-diamino-*m*-terphenyl (TPD).

(triphenylphospine)palladium catalyst was added, and 10 min later the gas inlet tube was removed, and a gentle flow of argon was introduced on top of the condenser. This mixture was heated to reflux (oil bath temperature of 70 °C) for 24 h. When the reaction was complete, the now dark colored mixture was cooled down to 25 °C and precipitated in 600 mL of ice water. A yellow precipitate was filtered off and washed with ethanol. The solid crude product was recrystallized twice from DMF. Pale yellow crystals were obtained and dissolved in DCM with charcoal to remove any remaining impurities, this mixture was filtered over Celite, and silica and the product was obtained as a white powder. Yield 5.33 g (55%); TLC: (9/1 hexane/ethyl acetate) $t_r = 0.622$ (one spot). GC/MS *m/z* (relative intensity) $t_R = 22.2$ min, 320 (100%).

4,4″-Diamino-m-terphenyl (TPD). A 250 mL hydrogenation bottle was charged with 5.33 g (0.017 mol) of 4,4″-dinitro-m-terphenyl, 150 mL of dry THF, and 0.29 g of 10% palladium on carbon. After degassing with argon for 20 min, the bottle was placed in a Parr hydrogenator, and the nitro groups were reduced under hydrogen atmosphere at 50 psi for 2 h at room temperature, then the shaker was turned off and the mixture was left under the same conditions of pressure and temperature overnight. The solution was filtered over Celite and the THF was removed by rotary evaporation. Pure TPD was obtained after two recrystallizations from ethanol/water (90/10) as pale brown crystals. Yield: 2.8 g (52%); mp: $T_{onset} = 151$ °C, $T_{max} = 161$ °C. TLC (9/1 hexane/ethyl acetate) $t_r = 0$ (one spot). ^{1}H NMR (DMSO-d_6, 400 MHz) δ (ppm): 7.64 (s, 1H), 7.41 (d, 4H, $J = 8$ Hz), 7.37 (t, 1H, $J = 4$ Hz), 7.36 (d, 2H, $J = 4$ Hz), 6.65 (d, 4H, $J = 8$ Hz), 5.21 (s, 4H); ^{13}C NMR (DMSO-d_6, 100 MHz) δ (ppm): 114.63, 122.96, 123.33, 127.73, 128.16, 129.51, 141.57, 168.48. GC/MS *m/z* (relative intensity) $t_R = 18.35$ min, 260 (100%).

The phthalic dianhydride with an 1,3,4-oxadiazole core (ODDA) was synthesized according to a method found in a patent by Palaniswamy et al. [21] Here, benzenetricarboxylic anhydride was reacted with hydrazine, forming a heterocyclic 1,3,4-oxadiazole ring (Scheme 2).

4,4'-(1,3,4-Oxadiazole-2,5-diyl)diphthalic anhydride (ODDA). A 250 mL three-neck round-bottom flask, equipped with a stirring bar, condenser and a nitrogen inlet, was charged with 29.62 g of 1,2,4-benzenetricarboxylic anhydride (154 mmol) and 80 mL of fuming sulfuric acid (65% free SO_3). This suspension was heated to 80 °C and stirred under nitrogen until all solid were dissolved, after which 9.56 g (73 mmol) of hydrazine sulfate salt was added in portions. The reaction mixture was heated and stirred at 90 °C for 4 h. The reaction mixture was poured onto crushed ice and the white precipitate was filtered off. White sticky solids were washed with water and filtered several times until the pH was neutral. The white solids were combined in a flask containing 50 mL of toluene so that the residual water could be removed by azeotropic distillation. The solids were dried for 48 h in a vacuum oven at 60 °C, after which recrystallization from acetic anhydride (50 mL/g) yielded the desired product as pure white crystals. Yield: 7.91 g (26.7%); mp: $T_{onset} = 322$ °C, $T_{max} = 326$ °C (326 °C).[21] ^{1}H NMR (DMSO-d_6, 400 MHz) δ (ppm): 8.32 (d, 2H, $J = 8$ Hz), 8.70 (d, 2H, $J = 6.8$ Hz), 8.92 (s, 2H); ^{13}C NMR (DMSO-d_6, 100 MHz) δ (ppm): 123.29, 123.47, 126,29, 129.54, 132.72, 133.82, 162.37, 162.44, 163.50.

2.4. Polymer synthesis

Polyamic acids of high molecular weight were prepared from the dianhydride and diamine monomers, in equimolar quantities, as 15 wt% solutions in NMP at 25 °C. *Preparation of ODDA-ODD 15 wt% polymer film (representative procedure,* Scheme 3*):* A dry 50 mL one-neck round-bottom flask was charged with 0.63 g (2.51 mmol) of 2,5-bis(4-aminophenyl)-1,3,4-oxadiazole (ODD) and 8 mL of dry NMP (water content <0.005%) was added. This solution was then stirred for 5 min, under a dry nitrogen flow, at room temperature with a magnetic stirrer at 120 rpm until the diamine monomer was dissolved. After this step the polymerization was initiated by adding 0.91 g (2.51 mmol, an equimolar amount) of 4,4'-(1,3,4-oxadiazole-2,5-diyl)diphthalic anhydride (ODDA), and the walls of the flask were washed with 2 mL of NMP. Polymerization was allowed to continue for 24 h under a dry nitrogen atmosphere, stirring at 90 rpm.

2.5. Film preparation

In order to remove any solid particles, the polyamic acid solution was filtered using a Sartorius pressure filter (0.45 μm). The resulting filtered solution was degassed to remove bubbles and then cast with a doctor-blade onto a clean, dry glass plate (film thickness ~0.6 mm) and placed in a clean vacuum oven at 60 °C for 1.5 h. Films were thermally imidized by heating to 100 °C for 1 h, 200 °C for 1 h, and 300 °C for 1 h. After cooling to 25 °C, the film was released from the glass plate by placing it in lukewarm water. All PIs were obtained as free-standing films using this procedure.

Matrimid® film preparation. 0.62 g of Matrimid® 5218 powder was dissolved in 4 mL of NMP, this solution was cast with a doctor-blade onto a clean, dry glass plate and was subjected to the same thermal program as described above for other polymers of this series. A free-standing film

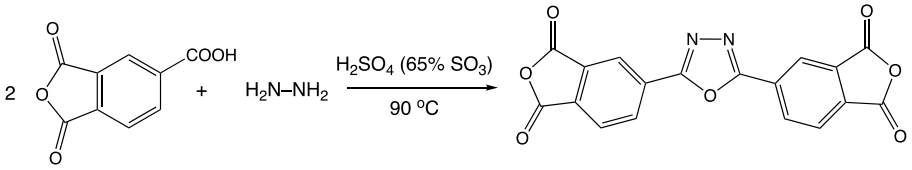

Scheme 2. Synthesis of 4,4'-(1,3,4-oxadiazole-2,5-diyl)diphthalic anhydride (ODDA).

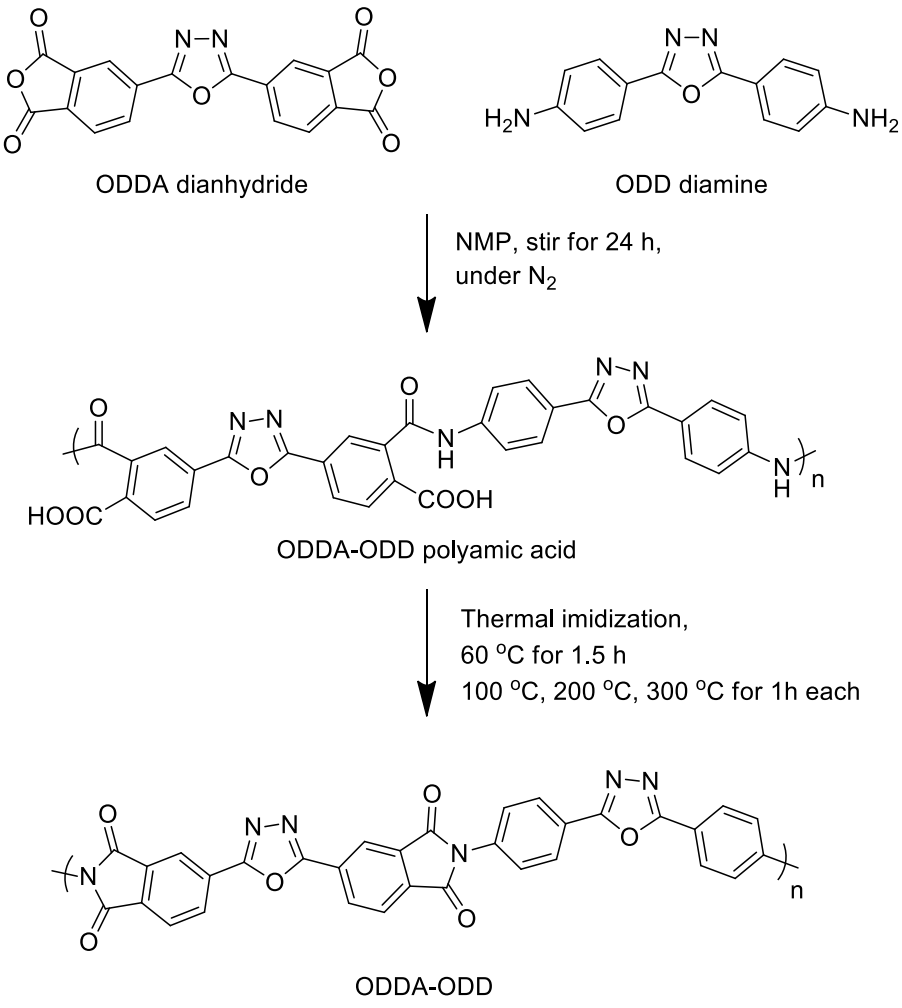

Scheme 3. Polymerization procedure used to prepare an ODDA-ODD free-standing membrane.

was obtained and used for gas permeation measurements as a reference membrane.

2.6. Gas permeation measurements

Gas permeation experiments were performed at the Catalysis Engineering Department of the TU-Delft, using an in-house built setup described elsewhere [22] and depicted in the Supporting Information (Scheme S1). An equimolar CO_2/CH_4 mixture was used as feed (50 mL/min of CO_2 and 50 mL/min of CH_4), while helium (67.7 mL/min) was used as sweep gas for the permeate flow. The absolute pressure of the feed stream was adjusted in a range of 3 bar–12 bar using a back-pressure controller at the retentate side. The temperature in the permeation module was kept constant and equal to 35 °C. The composition of the permeate flow was periodically measured using an on-line gas chromatograph (Interscience Compact GC) equipped with a packed Carboxen 1010 PLOT (30 m × 0.32 mm) column, a thermal conductivity detector (TCD) and a flame-ionization detector (FID). Digital flow meters measured the gas flows. Separation selectivity and gas permeability values are reported after a steady operating regime was reached. Experiments were performed at 4 different pressures at 3, 6, 9 and 12 bar. Permeability coefficients were calculated from the steady-state pressure increase $\Delta P_p/\Delta t$ with Eq. (I):

$$P_i = \frac{\varphi_{ni} \times \delta}{\Delta p_i \times A} \quad \text{(I)}$$

where φ_{ni} is the molar flow rate of the *i*-component, δ is the thickness of the membrane, Δp_i is the partial pressure difference of the *i*-component across the membrane and A is the membrane area. The SI unit for the permeability is mol s^{-1} m^{-1} Pa^{-1}. Still, permeabilities are commonly reported in non-SI unit Barrer, where 1 Barrer = 3.35×10^{-16} mol s^{-1} m^{-1} Pa^{-1}.

$$\alpha_{CO_2/CH_4} = \frac{P_{CO2}}{P_{CH4}} \quad \text{(II)}$$

The selectivity (α) was calculated as the ratio of permeabilities of two components, with Eq. (II):

Where P_{CO2} and P_{CH4} are permeabilities of CO_2 and CH_4, respectively. All membranes were cut to fit the module, their area determined to be 4.16 cm^2.

3. Results and discussion

3.1. Gel permeation chromatography measurements

The molecular weights of the polyamic acid intermediates, measured using GPC, are listed in Table 1 (GPC curves are shown in the SI). High molecular weight polyamic acids could be prepared without difficulties, with number average molecular weights in the range of 33,000 to 110,000 g/mol and polydispersities (PDI) of 1.5–2.9, which are typical values for step-growth polymers. All GPC curves show a unimodal molecular weight distribution (Figs. S1–S3). Tough, flexible and easy-to-handle PI films were obtained after thermal imidization. 6FDA gives

Table 1
Molecular weight and polydispersity data of the polyamic acids as determined by GPC.

	M_n (g/mol)	M_w (g/mol)	PDI = M_w/M_n
6FDA-TPD	42,000	64,000	1.5
6FDA-ODD	59,000	110,000	1.9
ODPA-TPD	110,000	319,000	2.9
ODPA-ODD	33,000	61,000	1.9
ODDA-TPD	101,000	229,000	2.2
ODDA-ODD	76,000	143,000	1.9

clear pale-yellow films, while ODPA and ODDA give darker yellow films, respectively. All polyamic acids were prepared at 15 wt% solids.

3.2. Dynamic thermogravimetric analysis

The thermal stability of all 6 PI films was investigated by dynamic thermogravimetric analysis. Sample films were cleaned and degreased with ethanol and dried at 60 °C for 2 h. All films were investigated under inert (nitrogen) conditions using a heating rate of 10 °C/min. This provided information with respect to the polymer decomposition temperature, the temperature at which a weight loss of 5% occurs ($T_d^{5\%}$) as well as the char yield at 595 °C. The resulting thermograms, showing polymer weight as a function of temperature, are shown in the SI (Figs. S4–S6) and the values for $T_d^{5\%}$ and char yield are listed in Table 2. The highest thermal stability is displayed by ODPA-TPD and 6FDA-TPD. TPD is an all-aromatic phenylene-based monomer and hence exhibits superior thermal stability. The values reported in Table 2 are typical for all-aromatic PEI- and PI-containing heterocycles [23–25]. As the PI-based membranes will operate at or slightly above 25 °C the thermal stability of this series will not be an issue.

3.3. Differential scanning calorimetry

The thermal properties of the PI films were determined by DSC using a PerkinElmer Sapphire DSC. Samples were heated at a rate of 20 °C/min under a nitrogen atmosphere to ~400 °C, depending on the thermal stability of the sample as determined by TGA. The DSC curves, first heats only, are shown in Fig. 2 and the T_g values are summarized in Table 2. We were unable to detect a T_g for ODPA-ODD as well as the ODDA-based series by DSC.

In general, incorporation of 6FDA groups in PI's and PEIs results in amorphous membranes [26] as the bulky CF3 groups that constitute 6FDA are effective in disrupting chain-chain packing preferences. Moreover, they also hinder chain rotation i.e. cooperative segmental motion is restricted, resulting in PIs with the highest T_gs and the largest free volume content. A trend in T_g could not be observed as it was difficult to determine the T_g for the ODDA-based series and ODPA-ODD. Although no visible melt peaks are observable by DSC for ODPA- and ODDA-series, DMTA and X-ray studies were performed to evaluate the polymer morphology; in many highly aromatic polyimides (e.g. Kapton™), melt-transitions often occur above T_d and cannot be measured by DSC.

Table 2
Thermal and mechanical properties of the polyimides.

Polymer	TGA[a]		DSC[b]	DMTA	
	5% weight loss (°C)	char yield at 595 °C (%)	T_g (°C)	T_g (°C)[c]	E' (GPa)[e]
6FDA-TPD	527	81	338	336	3.5
6FDA-ODD	478	69	356	352	4.7
ODPA-TPD	540	87	311	310	4.9
ODPA-ODD	437	64	–	276	4.3
ODDA-TPD	484	77	–	335	4.4
ODDA-ODD	452	64	–	320	4.2

[a] Heating rate 10 °C/min and nitrogen atmosphere.
[b] T_g is reported at the inflection point (heating rate 20 °C/min).
[c] T_g reported as the maximum of the loss modulus (E″)(heating rate of 2.5 °C/min).
[e] Storage modulus (E′) at 30 °C.

3.4. Dynamic mechanical thermal analysis

All DMTA curves are summarized in Fig. 3. All polyimide films are flexible and can be creased without breaking (Fig. S7) enabling thermomechanical analysis in tensile mode. The PI films show storage moduli (E') in the range of 3.5–4.9 GPa (Table 2), which is typical for all-aromatic PIs [23,27].

The storage modulus (E′) for the 6FDA-based PI films is typical for what is observed for amorphous polyimides—a sharp drop in E′ of ~4 orders of magnitude above the T_g (Fig. 3A1). The T_g values as determined by DMTA (peak in the loss modulus) corresponds well with the T_g values observed by DSC. A similar E′ behavior is observed for the ODPA-TPD film confirming an amorphous morphology (Fig. 3B1). However, above T_g, the E' for ODPA-ODD (Fig. 3B1) and both ODDA-based films (Fig. 3C1) plateaus at ~0.1 GPa i.e., 3 orders of magnitude larger than the amorphous 6FDA-based films. Moreover, the E" peak at the T_g is visibly suppressed (Fig. 3B2 and 3C2), which is typical for semi-crystalline polymers or polymers with rigid amorphous phases [28]. Together with the DSC results, this strongly suggests that the polymer morphology of ODPA-ODD and both ODDA-based films is different from both 6FDA- and the ODDA-TPD based films.

3.5. X-ray diffraction

All imidized PI films were characterized using X-ray diffraction. 6FDA- and ODDA-based films are fully amorphous (Fig. 4A), which agrees with our DSC results. The 1-D scattering curves are broad, which is consistent with an amorphous morphology with nominal peaks at 18° (d = 4.9 Å) and 27.5° (3.2 Å). These two distances have been reported previously for aromatic PI's and correspond to interchain distances [29,30]. The ODPA-TPD film is amorphous, however the ODPA-ODD film exhibits several sharp Bragg reflections (at 19° (d = 4.7 Å), 22° (4.0 Å), 26.5° (3.4 Å), and 29.5° (3.0 Å)) implying a high degree of crystalline order (Fig. 4B) [29]. This is consistent with the DMTA data and also implies that the crystal melting temperature is above 400 °C. The WAXD data for the ODDA-series are shown in Fig. 4C and indicate that both films are amorphous –both exhibit broad peaks at ~19° (4.7 Å) and ~29.5° (3.2 Å).

3.6. Gas permeation and separation experiments

The gas separation performance of this polyimide membrane series, including the reference material Matrimid®, have been assessed with permeation experiments performed at 3, 6, 9 and 12 bar of equimolar CO_2/CH_4 feed at 35 °C. Values for CO_2 permeability and mixed gas selectivity are reported after a steady operating regime was reached. Fig. 5 shows the CO_2 permeabilities of the 6 PI membranes and Matrimid® as a function of the mixed feed pressure at 35 °C. The data is grouped by dianhydride moiety for sake of clarity.

It is a well-known fact that the introduction of a $-C(CF_3)_2-$ bridge into the polyimide backbone effectively improves permeability as well as selectivity for different gas pairs [9,14]. As expected, our permeation experiments show that both 6FDA-based PIs have the highest permeabilities in this whole series. CO_2 permeability coefficients as a function of feed pressure for 6FDA-based PIs are shown in Fig. 5A alongside the commercial membrane Matrimid®. The 6FDA-ODD membrane shows

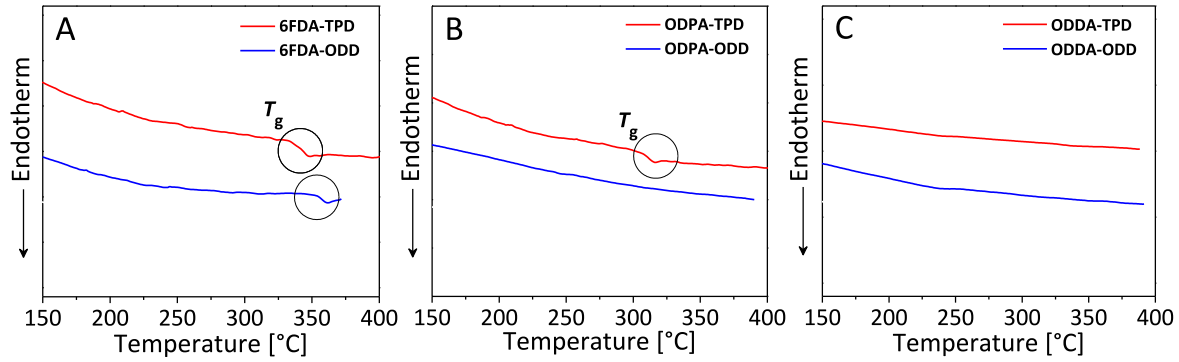

Fig. 2. DSC curves showing the T_g events as a function of temperature. (A) 6FDA-series, (B) ODPA-series and (C) ODDA-based PI series. First heat, recorded under a N_2 atmosphere at 20 °C/min. All curves have been normalized to sample weight and translated vertically for sake of clarity.

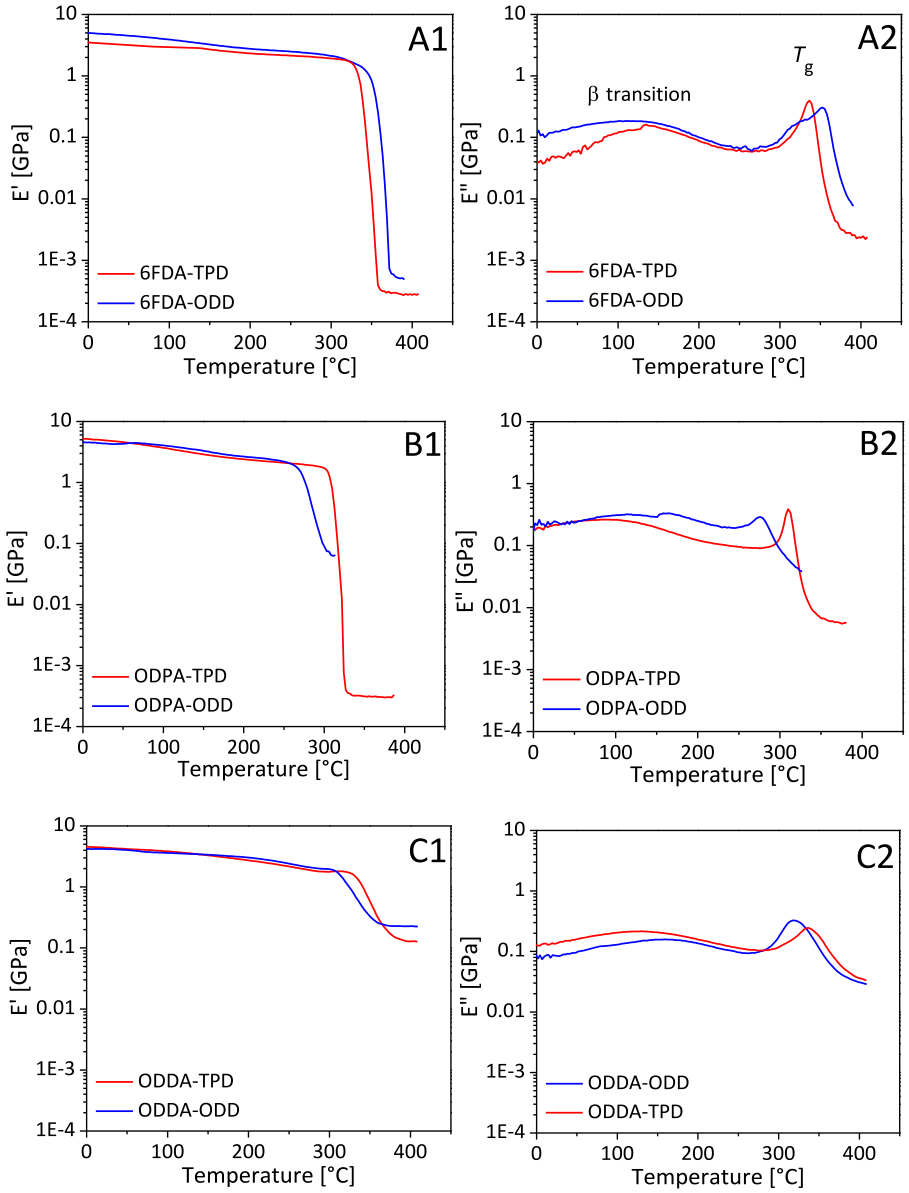

Fig. 3. DMTA results of the fully imidized PI films. The storage moduli (E′) and loss moduli (E″) were recorded as a function of temperature (N_2 atmosphere at a frequency of 1 Hz and a heating rate of 2.5 °C/min). (**A**) 6FDA-series, (**B**) ODPA-series and (**C**) ODDA-based PI series.

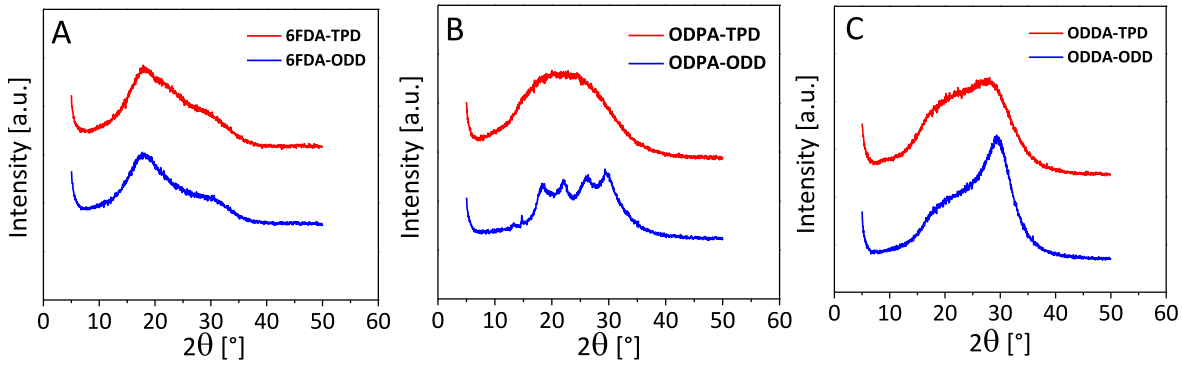

Fig. 4. XRD results of the fully imidized PI films. The intensity is plotted as a function of the scattering angle. All curves have been translated vertically for sake of clarity. (**A**) 6FDA-series, (**B**) ODPA-series and (**C**) ODDA-series.

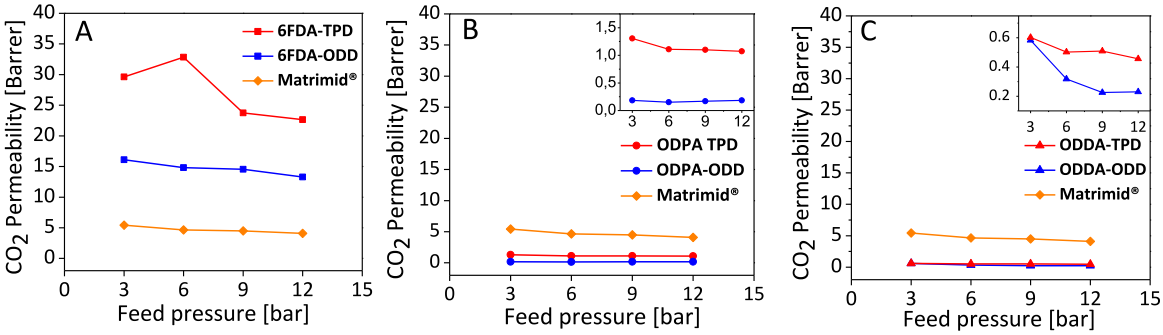

Fig. 5. CO_2 permeability as a function of the mixed feed pressure at 35 °C. (**A**) 6FDA-series, (**B**) ODPA-series and (**C**) ODDA-based membrane series. Matrimid® is included for reference purposes. Feed mixed gas: CO_2/CH_4 (50/50 vol%). Based on duplicate measurements of the membranes, error for permeability was found to range between 1.77 and 2.94%. Error bars are not shown in the figure.

excellent membrane performance with high CO_2 permeability values at all feed pressures. With P_{CO2} of 16 Barrer at 3 bar it is 3 times more permeable than the commercial reference Matrimid® membrane. For both 6FDA-ODD and Matrimid® P_{CO2} decreases steadily with increasing feed pressure. This decrease in permeability comes from the decreasing solubility with increasing pressure, following the predicted behavior of glassy polymers described by the dual-mode sorption model [8,31]. It is expected that, above our measurement maximum of 12 bars, P_{CO2} would reach a minimum at a certain pressure *i.e.* the plasticization pressure [32,33]. The slight downward trend of mixed gas selectivity confirms this (Fig. 5A). The effect of having a 6FDA moiety in the PI backbone on the increase in gas permeability is clear. At the same time, it is also apparent that a subtle change introduced in the diamine structure amounts to a large P_{CO2} difference as well. Throughout the whole pressure range, 6FDA-TPD displays superior performance in CO_2 permeability. At 3 bar of mixed feed 6FDA-TPD has a CO_2 permeability of 30 Barrer, almost 2 times that of 6FDA-ODD and 6 times that of commercial Matrimid®. With an increase in feed pressure, 6FDA-TPD shows a somewhat unexpected behavior with an initial P_{CO2} increase (33 Barrer at a feed pressure of 6 bar), followed by a drop to 23 Barrer.

Both ODPA- and ODDA-based membranes have significantly lower CO_2 permeabilities than the 6FDA-series. In the ODPA-based series (Fig. 5B) the ODPA-TPD membrane shows a CO_2 permeability of 1.25 Barrer and the ODPA-ODD membrane shows a CO_2 permeability of 0.25 Barrer (over a feed pressure range of 6–12 bar). In terms of CO_2 permeability, both membranes perform well below the Matrimid® reference membrane. Remarkably both ODDA-TPD and ODDA-ODD membranes display virtually the same performance over the whole feed pressure range (Fig. 5C). The ODDA-TPD membrane shows a CO_2 permeability of ~0.5 Barrer and the ODDA-ODD membrane shows a CO_2 permeability of ~0.2 Barrer. From these results it is clear that when both diamines are coupled with the 6FDA dianhydride, high CO_2 permeabilities can be achieved whereas selecting ODPA or ODDA a significant reduction in CO_2 permeability results. A trend that emerges is that P_{CO2} decreases in the following order: 6FDA ≫ ODPA ≥ ODDA.

The gas separating performance of our new PI membranes is summarized in Fig. 6. The values for CO_2/CH_4 selectivities as a function of the partial gas pressure at 3, 6, 9 and 12 bar are presented and grouped by the dianhydride moiety for sake of clarity.

The 6FDA-ODD membrane displays the highest selectivity of all membranes tested and surpasses Matrimid® (Fig. 6A). 6FDA-ODD exhibits a CO_2/CH_4 selectivity of 47 at 3 bar of mixed feed, which decreases steadily to 40 at 12 bar. At a feed pressure of 3 bar, 6FDA-ODD is 40% more selective than Matrimid®. Both 6FDA-ODD and Matrimid® show a slight downward slope indicating imminent plasticization pressure around 12 bar and higher. In terms of separating ability, the 6FDA-TPD membrane is comparable to Matrimid® with stable values for selectivity around 30 over the whole pressure range. The ODPA-based membranes, on the other hand, show unusually low selectivities for PI-based membranes. ODPA-TPD is two times more selective than its oxadiazole containing counterpart (ODPA-ODD), but these values are still only around 20 for the entire pressure range. The ODDA-based membrane displays interesting behavior in that the ODDA-TPD membrane shows a moderate increase in selectivity (from 12 to 17) as the function of increasing feed pressure. Such an increase in selectivity is observed for all TPD-based polyimide membranes. We speculate this is due to strong adsorption of CO_2 at elevated pressures that results in the blocking of methane from permeating through the membrane. Similar examples have been reported for other membrane materials such as zeolites. [34] In contrast, the ODDA-ODD membrane shows a selectivity of 17 at a feed pressure of 3 bar but upon increasing the feed pressure the selectivity drops rapidly to 8 (feed pressure of 12 bar) as a result of

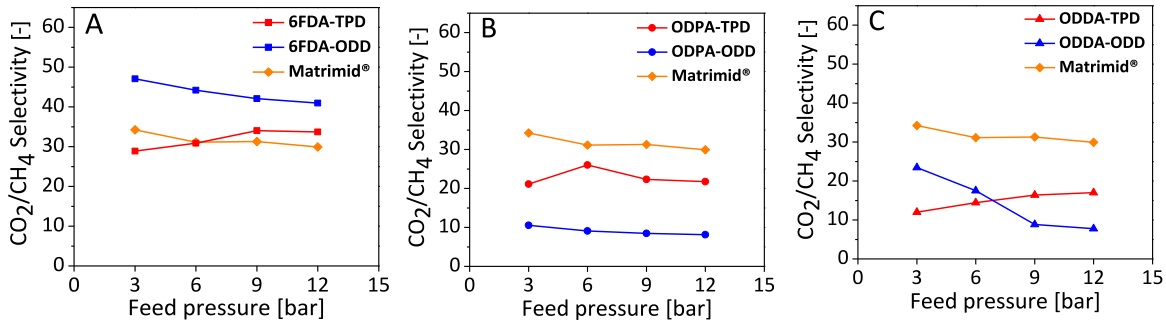

Fig. 6. CO_2/CH_4 selectivity as function of feed pressure. (**A**) 6FDA-series, (**B**) ODPA-series and (**C**) ODDA-based membrane series. Matrimid® is included for reference purposes. Feed mixed gas: CO_2/CH_4 (50/50 vol%).

plasticization. None of the ODPA- or ODDA-based membranes are able to outperform Matrimid® under the test conditions used.

4. Conclusions

A new series all-aromatic polyimide (PI) membranes was prepared with the aim to understand how the backbone geometry and the local electrostatic dipole moments govern gas transport properties in PI-based membranes. All PIs exhibit high glass transition temperatures (T_g > 270 °C), high thermal stability ($T_{d5\%}$ > 450 °C) and excellent mechanical properties (E' ~ 4 GPa at 30 °C). The 6FDA-based membranes showed high CO_2 permeability, ranging from 4 to 30 Barrer. The best performing membrane of the series is 6FDA-TPD. At mixed feed pressure of 3 bar, 6FDA-TPD has a CO_2 permeability of 30 Barrer, which is almost 2 × that of 6FDA-ODD, and 6 × that of Matrimid®. With respect to selectivity, 6FDA-TPD is comparable to Matrimid®, demonstrating values of around 30 throughout the applied pressure range. The optimum pressure for the application of 6FDA-TPD and 6FDA-ODD would be between 3 and 6 bar, where they show a P_{CO2} of 33 and 15 Barrer, and CO_2/CH_4 selectivity of 31 and 44 respectively. Unlike single gas permeation experiments, mixed feed tests unequivocally demonstrate that these membranes are able to operate using a 50/50 vol% CO_2/CH_4 feed. When we contrast the selectivity performance of the polar ODD-based PI series with the non-polar TPD-based PI series, we can conclude that the strong dipole moment (3D) associated with the 1,3,4-oxadiazole heterocycle governs the high selectivity in the ODD-based PI membranes based on 6FDA and ODDA dianhydrides, i.e. amorphous ODD-based polyimides. We speculate that the rigidity of the anhydride monomers (6FDA and ODDA) prevents plasticization and therefore an adsorption diffusion mechanism of permeation dominates over the classical solution diffusion mechanical predominant in pure polymeric membranes. In terms of permeability, we found that the backbone geometry dominates.

CRediT authorship contribution statement

Zeljka P. Madzarevic: Formal analysis, Investigation, Methodology, Writing – review & editing. **Beatriz Seoane:** Formal analysis, Investigation, Writing – review & editing. **Jorge Gascon:** Supervision, Writing – review & editing. **Maruti Hegde:** Methodology, Writing – review & editing. **Theo J. Dingemans:** Conceptualization, Supervision, Funding acquisition, Writing – review & editing.

Declaration of competing interest

The authors declare that they have no known competing financial interests or personal relationships that could have appeared to influence the work reported in this paper.

Data availability

Data will be made available on request.

Acknowledgment

This research forms part of the research program of the Dutch Polymer Institute (DPI), project #715.

Appendix A. Supplementary data

Supplementary data to this article can be found online at https://doi.org/10.1016/j.polymer.2022.125520.

References

[1] L.M. Robeson, Correlation of separation factor versus permeability for polymeric membranes, J. Membr. Sci. 62 (2) (1991) 165–185.
[2] L.M. Robeson, The upper bound revisited, J. Membr. Sci. 320 (1–2) (2008) 390–400.
[3] S.M. Allen, M. Fujii, V. Stannett, H.B. Hopfenberg, J.L. Williams, The barrier properties of polyacrylonitrile, J. Membr. Sci. 2 (1977) 153–163.
[4] T.C. Merkel, V.I. Bondar, K. Nagai, B.D. Freeman, I. Pinnau, Gas sorption, diffusion, and permeation in poly(dimethylsiloxane), J. Polym. Sci., Part B: Polym. Phys. 38 (2000) 415–434.
[5] Y. Yampolskii, Polymeric gas separation membranes, Macromolecules 45 (2012) 3298–3311.
[6] D. Ayala, A.E. Lozano, J. de Abajo, C. Garcia-Perez, J.G. de la Campa, K.-V. Peinemann, B.D. Freeman, R. Prabhakar, Gas separation properties of aromatic polyimides, J. Membr. Sci. 215 (2003) 61–73.
[7] B.D. Freeman, N. Carolina, Basis of permeability/selectivity tradeoff relations in polymeric gas separation membranes, Macromolecules 32 (1999) 375–380.
[8] S. Alexander Stern, Polymers for gas separations: the next decade, J. Membr. Sci. 94 (1994) 1–65.
[9] M.R. Coleman, W.J. Koros, Isomeric polyimides based on fluorinated dianhydrides and diamines for gas separation applications, J. Membr. Sci. 50 (1990) 285–297.
[10] P.M. Budd, N.B. McKeown, D. Fritsch, Y. Yampolskii, V. Shantarovich, Chapter 2, in: Y. Yampolskii, B.D. Freeman (Eds.), Membrane Gas Separation, John Wiley & Sons, Chichester, UK, 2010, p. 29.
[11] M.L. Cecopieri-Gomez, J. Palacios-Alquisira, J.M. Dominguez, On the limits of gas separation in CO_2/CH_4, N_2/CH_4 and CO_2/N_2 binary mixtures using polyimide membranes, J. Membr. Sci. 293 (2007) 53–65.
[12] D.F. Sanders, Z.P. Smith, R. Guo, L.M. Robeson, J.E. McGrath, D.R. Paul, B. D. Freeman, Energy-efficient polymeric gas separation membranes for a sustainable future: a review, Polymer 54 (2013) 4729–4761.
[13] C. Zhang, B. Cao, P. Li, Thermal oxidative crosslinking of phenolphthalein-based cardo polyimides with enhanced gas permeability and selectivity, J. Membr. Sci. 546 (2018) 90–99.
[14] S.K. Sen, B. Dasgupta, S. Banerjee, Effect of introduction of heterocyclic moieties into polymer backbone on gas transport properties of fluorinated poly(ether imide) membranes, J. Membr. Sci. 343 (2009) 97–103.
[15] J.R. Fried, N. Hu, The molecular basis of CO_2 interaction with polymers containing fluorinated groups: computational chemistry of model compounds and molecular simulation of poly[bis(2,2,2-trifluoroethoxy)phosphazene], Polymer 44 (2003) 4363–4372.
[16] M. Calle, A.E. Lozano, J. de Abajo, J.G. de la Campa, C. Álvarez, Design of gas separation membranes derived of rigid aromatic polyimides. 1. Polymers from diamines containing di-tert-butyl side groups, J. Membr. Sci. 365 (2010) 145–153.

[17] M. Lehmann, J. Seltmann, A.A. Auer, E. Prochnow, U. Benedikt, Synthesis and mesomorphic properties of new V-shaped shape-persistent nematogens containing a thiazole or a thiadiazole bending unit, J. Mater. Chem. 19 (2009) 1978–1988.
[18] Z.P. Madzarevic, S. Shahid, K. Nijmeijer, T.J. Dingemans, The role of ortho-, meta- and para-substitutions in the main-chain structure of poly(etherimide)s and the effects on CO_2/CH_4 gas separation performance, Separ. Purif. Technol. 210 (2019) 242–250.
[19] M. Grucela-Zajac, M. Filapek, L. Skorka, K. Bijak, K. Smolarek, S. Mackowski, E. Schab-Balcerzak, Photophysical, electrochemical and thermal properties of new (Co)polyimides incorporating oxadiazole moieties, Synth. Met. 188 (2014) 161–174.
[20] D.J. Sinclair, M.S. Sherburn, Single and double suzuki-miyaura couplings with symmetric dihalobenzenes, J. Org. Chem. 70 (2005) 3730–3733.
[21] G. Palaniswamy, F. Hannour, T.J. Dingemans, R. Bouwer, Organic Solar Cell of the Bulk Heterojunction Type Comprising an Imide Based Conjugated Backbone Compound as Photoactive Amterial, World Intellectual property Organization, 2014. Patent number *WO2014 000850 A1*.
[22] B. Zornoza, A. Martinez-Joaristi, P. Serra-Crespo, C. Tellez, J. Coronas, J. Gascon, F. Kapteijn, Functionalized flexible MOFs as fillers in mixed matrix membranes for highly selective separation of CO_2 from CH_4 at elevated pressures, Chem. Commun. 47 (2011) 9522–9524.
[23] T.J. Dingemans, E. Mendes, J.J. Hinkley, E.S. Weiser, T.L. Stclair, Ortho-arylene substitutions: synthesis, characterization and liquid crystalline properties, Macromolecules 41 (2008) 2474–2483.
[24] M. Grucela-Zajac, M. Filapek, L. Skorka, K. Bijak, K. Smolarek, S. Mackowski, E. Schab-Balcerzak, Photophysical, electrochemical and thermal properties of new (Co)polyimides incorporating oxadiazole moieties, Synth. Met. 188 (2014) 161–174.
[25] Y. Mansoori, M. Ghanbari, Novel polyimides obtained from a new aromatic diamine (BAPO) containing pyridine and 1,3,4-oxadiazole moieties for removal of Co(II) and Ni(II) ions, Polym. Adv. Technol. 26 (2015) 658–664.
[26] Z.P. Smith, D.F. Sanders, C.P. Ribeiro, R. Guo, B.D. Freeman, D.R. Paul, J. E. McGrath, S. Swinnea, Gas sorption and characterization of thermally rearranged polyimides based on 3,3′-dihydroxy-4,4′-diamino-biphenyl (HAB) and 2,2′-bis-(3,4-dicarboxyphenyl) hexafluoropropane dianhydride (6FDA), J. Membr. Sci. 415–416 (2012) 558–567.
[27] M. Ding, Isomeric polyimides, Prog. Polym. Sci. 32 (2007) 623–668.
[28] M. Hegde, E.T. Samulski, M. Rubinstein, T.J. Dingemans, The role of crystallinity in SWCNT–polyetherimide nanocomposites, Compos. Sci. Technol. 110 (2015) 176–187.
[29] K. Takizawa, J. Wakita, S. Azami, S. Ando, Relationship between molecular aggregation and optical properties of polyimide films analyzed by synchotron wide-angle X-ray diffraction, in frared absorption, and UV/visible absorption spectroscopy at very high pressure, Macromolecules 44 (2011) 349–359.
[30] J. Wakita, S. Jin, T.J. Shin, M. Ree, S. Ando, Analysis of molecular aggregation structures of fully aromatic and semialiphatic polyimide films with synchrotron grazing incidence wide-angle X-ray scattering, Macromolecules 43 (2010) 1930–1941.
[31] D.R. Paul, Gas sorption and transport in glassy polymers, Ber. Bunsenges. Phys. Chem 83 (1979) 294–302.
[32] T. Visser, M. Wessling, When do sorption-induced relaxations in glassy polymers set in? Macromolecules 40 (2007) 4992–5000.
[33] V. Stannett, The transport of gases in synthetic polymeric membranes - an historic perspective, J. Membr. Sci. 3 (2) (1978) 97–115, https://doi.org/10.1016/S0376-7388(00)83016-1.
[34] J. van den Bergh, W. Zhu, J. Gascon, J.A. Moulijn, F. Kapteijn, Separation and permeation characteristics of a DD3R zeolite membrane, J. Membr. Sci. 316 (2008) 35–45.